

Article

# Selection of a PCM for a Vehicle's Rooftop by Multicriteria Decision Methods and Simulation

Juan Francisco Nicolalde <sup>1,\*</sup>, Mario Cabrera <sup>1</sup>, Javier Martínez-Gómez <sup>1,2</sup>, Rodger Benjamín Salazar <sup>3</sup> and Evelyn Reyes <sup>1</sup>

<sup>1</sup> Facultad de Ingeniería y Ciencias Aplicadas, Universidad Internacional SEK, Quito 170302, Ecuador; mcabrera.mec@uisek.edu.ec (M.C.); javier.martinez@uisek.edu.ec (J.M.-G.); epreyes.mee@uisek.edu.ec (E.R.)

<sup>2</sup> Instituto de Investigación Geológico y Energético (IIGE), Quito 170518, Ecuador

<sup>3</sup> Facultad de Ciencias de la Ingeniería, Universidad Técnica Estatal de Quevedo, Quevedo 120301, Ecuador; rsalazarl@uteq.edu.ec

\* Correspondence: juan.nicolalde@uisek.edu.ec

**Featured Application:** Energy efficiency and thermal comfort on vehicles.

**Abstract:** The automotive industry is one of the most contaminant; for this reason, solutions in efficient matter has been proposed over the years. This research contributes to this subject by evaluating the thermal comfort in the internal air of a vehicle by using a 20 mm layer of a phase-change material attached to the rooftop interior of a car. The phase-change material selection is based on a list of other materials proposed in previous research and chosen by multicriteria decision methods. In this sense, the material savENRG PCM-HS22P proved to be the best. Moreover, a simulation using the finite elements method showed how the PCM reduced the temperature of the air by 9 °C when heating and by 4 °C when the temperature drops. To conclude, the multicriteria selection methods chose the best material to absorb energy during the charging process and released it during the discharging event in this automotive application.

**Keywords:** phase-change material; multicriteria decision; finite element; automotive; energy storage



**Citation:** Nicolalde, J.F.; Cabrera, M.; Martínez-Gómez, J.; Salazar, R.B.; Reyes, E. Selection of a PCM for a Vehicle's Rooftop by Multicriteria Decision Methods and Simulation. *Appl. Sci.* **2021**, *11*, 6359. <https://doi.org/10.3390/app11146359>

Academic Editor: Ioannis Kartsonakis

Received: 27 May 2021

Accepted: 24 June 2021

Published: 9 July 2021

**Publisher's Note:** MDPI stays neutral with regard to jurisdictional claims in published maps and institutional affiliations.



**Copyright:** © 2021 by the authors. Licensee MDPI, Basel, Switzerland. This article is an open access article distributed under the terms and conditions of the Creative Commons Attribution (CC BY) license (<https://creativecommons.org/licenses/by/4.0/>).

## 1. Introduction

The utilization of air conditioning and heating systems to control passengers' comfort in the automotive industry impacts the fuel consumption and economy, which makes it necessary to improve the fuel efficiency [1–3], where the internal temperature of the vehicle's air, as a measurable factor of discomfort, should be controlled between 23 °C and 28 °C [4]. In order to handle this, the development of energy-efficient solutions have been implemented, one of these being Thermal Energy Storage (TES), which is the most efficient in using the available heat resources [5,6]. In this sense, Latent Heat Storage (LHS) is responsible for the accumulation of energy. In phase-change materials (PCM), this phenomena takes place at a molecular level and triggers the transition between phases [7], producing an endothermic reaction when melting and an exothermic reaction when changing from liquid to solid [8]. In this sense, the performance of the PCM depends on the climate and the amount of PCM [9]. Moreover, when talking about LHS, PCMs are classified in organic PCMs, inorganic PCMs and eutectic mixtures; these last ones are mixes of two or more composites that melt and solidify together [10].

The utilization of PCMs has been widely studied for the properties presented during the phase change; in this sense, naming the research of Bakan et al., it has been established the importance of the crystallization during the phase change and the requirement to study the crystal growth in different temperature ranges. In this way, the crystal growth of the PCM  $\text{Ge}_2\text{Sb}_2\text{Te}_2$ , in a range of temperatures between 300 K and 870 K, has been studied [11], allowing to develop a PCM with promising nanophotonic applications that has

to be investigated [12]. Furthermore, the thermal applications of PCMs were investigated to reduce the indoor temperatures and reduce the internal air temperature to reach a maximum [13] by storing solar energy [14]. On the other hand, in the automotive industry, PCMs have been used as thermo stabilizers for batteries of electric and hybrid vehicles, by storing the overheat since natural and forced convection are not as efficient [6]. The size of the radiator and the cooling fan also can be reduced by using PCMs and help the cold ignite as well as recover the latent heat [15,16].

PCMs have a wide variety and different properties that are needed for different applications [17]; in this sense, multicriteria decision methods (MCDM) have been used in the selection of PCMs over several areas with great results. The methods used in this research are the Analytic Hierarchy Process [18], the Technique for Order Preference by Similarity to Ideal Solution (TOPSIS) [19], the VIKOR method [20] and the Complex Proportional Assessment Methods (COPRAS) [21]. Moreover, the selection by MCDM was validated by simulations of the superplastic forming for a vehicle's components [22], as well as the selection by MCDM and simulation to enhance the PCM by nanoparticles [23]. In this sense, finite elements analysis has been useful in automotive design, such as in disk brakes and its thermo-mechanical behavior [24].

The building industry has had a leading role in the research of simulated PCMs selected by MCDM, but the automotive sector does not much apply these tools for this benefit. With this previous knowledge, this research aims to select the best PCM by MCDM means based on a bibliographical research, to be applied in a 20 mm layer of PCM that will store energy in the charging process and release it in the discharging event to control the internal air temperature, and where this phenomenon will be simulated by computer-aided engineering.

## 2. Materials and Methods

### 2.1. Materials Determination

Rastogi et al. did a research where 35 PCMs passed through a MCDM selection, where the candidates were considered for heating, ventilation and air-conditioning application in buildings; also in this investigation, the author takes in consideration the Figures of Merit (FOMs), for the performance of the heat extraction per unit volume (FOM1) and the response time of the material (FOM2). Thus, these criteria will be used as the base, where 15 with the best specific heat capacity will be considered for the MCDM proposed for automotive rooftop applications. However, in this selection, some materials from the same family have the same specific heat capacity; for these materials, the one with the best heat extracted per unit volume (FOM1) calculated is considered. In this way, the materials PlusICE PCM A22, PlusICE PCM A23, PlusICE PCM S19, PlusICE PCM S21, PlusICE PCM S25, Rubitherm GmbH PCM SP21E2, Rubitherm GmbH PCM SP25E2, Rubitherm GmbH PCM RT21, Rubitherm GmbH PCM RT24, Rubitherm GmbH PCM RT25, Rubitherm GmbH PCM RT27, Rubitherm GmbH PCM RT21HC and Rubitherm GmbH PCM RT22HC are rejected and, in the case of the materials Rubitherm GmbH PCM SP24E and Rubitherm GmbH PCM SP26E that have the same values, the series SP24E stands for its wide range of phase-change temperatures [25]. In this sense, Table 1 displays the materials considered with its thermal properties. Furthermore, it is important to point out that this investigation will use the lowest thermal phase-change temperature and characteristics in the liquid state; also, an M index was added to the materials as a label to be used in the MCDM to be used instead of the full name. On the other hand, Table 2 shows the results of the calculations made for the figures of merit [25].

### 2.2. Analytic Hierarchy Process (AHP)

For this automotive application, the following characteristics are searched for:

1. Phase change in an environment temperature;
2. Good density for a low volume change when changing phases;
3. Low fusion heat for a quick and efficient phase change;
4. High latent heat for efficient thermal storage;
5. Good thermal conductivity to transmit the thermal energy.

**Table 1.** List of phase-change materials and their thermo-physical properties.

Compound (M)		Phase-Change Temp (°C)	Density (kg/m <sup>3</sup> )	Heat of Fusion (kJ/kg)	Specific Heat Capacity (kJ/kgK)	Thermal Conductivity (W/mK)
RUBITHERM GmbH, PCM SP 24 E	M1	24–35	1500	190	2	0.6
PlusICE PCM, S23	M2	23	1530	175	2.2	0.54
savENRG PCM-HS24P	M3	24	1820	185	2.26	0.5–1.09
PUR-PCM, BASF Polyurethanes GmbH	M4	22	970	365	2	0.19
PlusICE PCM, S17	M5	17	1525	160	1.9	0.43
CoolZONE23, Armstrong	M6	21–22	770	342	2	0.2
savENRG PCM-HS22P	M7	23	1540	185	3.05	0.5–1.09
ThermalCORE 23 C/ 73 F, USA	M8	22–24	770	342	2.2	0.2
Weber.murclima 23, St. Gobain-weber	M9	22–24	950	170	2.32	0.38
RUBITHERM GmbH, PCM RT 25 HC	M10	22–26	880	230	2	0.2
PlusICE PCM, PCM, A25H	M11	25	810	226	2.15	0.18
PlusICE PCM, A22H	M12	22	820	216	2.85	0.18
PlusICE PCM, A25	M13	25	785	150	2.26	0.18
PlusICE PCM, A24	M14	24	790	145	2.22	0.18
PCM-Akustikputz 23, SchreffGmbH& Co.	M15	21–22	400	196	1.7	0.08

**Table 2.** FOMs results.

Compound (M)		FOM1*10 <sup>6</sup> ρ*L	FOM2*10 <sup>-6</sup> k/ρ*C <sub>p</sub>
RUBITHERM GmbH, PCM SP 24 E	M1	285	0.2
PlusICE PCM, S23	M2	267.75	0.16042
savENRG PCM-HS24P	M3	336.7	0.12161
PUR-PCM, BASF Polyurethanes GmbH	M4	354.05	0.09793
PlusICE PCM, S17	M5	244	0.14840
CoolZONE23, Armstrong	M6	263.34	0.12987013
savENRG PCM-HS22P	M7	284.9	0.10631
ThermalCORE 23 C/ 73 F, USA	M8	263.34	0.11806
Weber.murclima 23, St. Gobain-weber	M9	161.5	0.17241
RUBITHERM GmbH, PCM RT 25 HC	M10	202.4	0.11363
PlusICE PCM, PCM, A25H	M11	183.06	0.10335
PlusICE PCM, A22H	M12	177.12	0.07702
PlusICE PCM, A25	M13	117.75	0.101459
PlusICE PCM, A24	M14	114.55	0.10263428
PCM-Akustikputz 23, SchreffGmbH& Co.	M15	78.4	0.11764

These requirements are fulfilled by the candidates and the AHP method allows to weight them; this process is developed in the research of Odu. G.O. [26]. Moreover, the method requires a label for the criteria, which is displayed as follows:

- Phase-change Temp = T1;
- Density = T2;
- Heat of fusion= T3;
- Specific heat capacity = T4;
- Thermal conductivity = T5;
- FOM1 \* 10<sup>6</sup>ρ \* L = T6;
- FOM2 \* 10<sup>-6</sup>k/ρ \* C<sub>p</sub> = T7.

### 2.3. Method VIKOR

Following the method used by Shekhovtsov and Salabun [27], the VIKOR method solves selection problems looking for a ranking where the alternative and criteria that will be used is the solution closest to the ideal [28]. This method requires that the criteria described before have the following considerations:

- T1 Higher = Better;

- T2 Lower = Better;
- T3 Higher = Better;
- T4 Higher = Better;
- T5 Higher = Better;
- T6 Higher = Better;
- T7 Lower = Better.

With these in mind, the VIKOR method will be performed as the named previous research.

#### 2.4. TOPSIS Method

The TOPSIS method takes and classifies a finite number of alternatives by similarity to the ideal solutions, looking for the alternatives to have the shortest distance to the ideal positive solution and the farthest from the negative [28]. The steps proposed by Shekhovtsov and Salabun [27] are followed and the cost and profit criteria are the same that were determined by the VIKOR method.

#### 2.5. COPRAS-G Method

The ranking of the alternatives in the COPRAS method considers the utility degree of the different options by using grey numbers that comes from the grey theory for insufficient information [28]. This method is followed as in the research of Mousavi-nasab [29] and Sotoudeh-anvai [30], where the beneficial and non-beneficial criteria are defined as follows:

- T1 = Beneficial;
- T2 = Non-Beneficial;
- T3 = Beneficial;
- T4 = Beneficial;
- T5 = Beneficial;
- T6 = Beneficial;
- T7 = Non-Beneficial.

#### 2.6. Spearman's Correlation Coefficient

The different methods obtains different results; to measure the relation between these non-linear results, Spearman's correlation was used. In this sense, this technique quantifies the strength between the variables; if there are no duplicated data, the perfect correlation is +1 or -1. This was calculated following the research of Beltrán and Martínez-Gómez [28].

#### 2.7. Simulation

The simulation of the system takes into consideration the three solids that make up the rooftop of the vehicle, which is made by steel bake hardening, YS260, and cold rolling. This material is described as used for automotive applications, such as roofs, in the software CES-Granta Edupack [31]. The next body represents a layer of material that corresponds to the 20 mm PCM made of the selected material by the MCDM and finally air fills the space; the proposed geometry is displayed in Figure 1. On the other hand, the simulation took two events, the first when the roof is heating up and the PCM is storing energy and the second where the roof is cooling down and the PCM releases the stored energy.

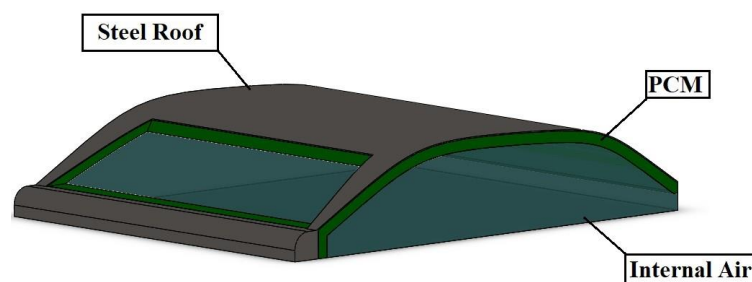


Figure 1. The CAD model.

### 2.8. Boundary Conditions

The simulation of the charging events comes with the parameters investigated by Dadour et al., who found that the temperature of a parked vehicle's black rooftop can start at 12 °C and rise to 45 °C, provoking a charge event [32]. On the other hand, after reaching this heating peak, a cooling process begins and the temperature reduces to 12 °C in 15 h. Where a discharging event takes place, these events are the ones that will be simulated [32]. Moreover, a convection process with a coefficient for free gases is found in the range of  $2 \frac{W}{m^2K}$  and  $25 \frac{W}{m^2K}$  [33]; for this reason, a middle value of  $12 \frac{W}{m^2K}$  will be used to simulate this phenomena. It is important to point out that the initial temperature of the air is the one reached in the charging event; the boundary conditions of these simulations are displayed in Tables 3 and 4 with the mesh data of the simulation.

**Table 3.** Boundary conditions for charge.

Element	Parameter
Roof Initial Temperature	12 °C
Roof Final Temperature	45 °C
Temperature Time Lapse	5 h
PCM Initial Temperature	12 °C
Internal Air Initial Temperature	12 °C
Environmental Temperature	24 °C
Convection coefficient	12 W/m <sup>2</sup> * K
Software	Solidworks 2020
Meshes	Blended curvature-based mesh
Mesh Quality	High
Jacobian Points	4
Max element size	22 mm

**Table 4.** Boundary conditions for discharge.

Element	Parameter
Roof Initial Temperature	45 °C
Roof Final Temperature	12 °C
Temperature Time Lapse	15 h
PCM Initial Temperature	40 °C
Internal Air Initial Temperature	37 °C
Environmental Temperature	24 °C
Convection coefficient	12 W/m <sup>2</sup> * K
Software	Solidworks 2020
Meshes	Blended curvature-based mesh
Mesh Quality	High
Jacobian Points	4
Max element size	22 mm

## 3. Results and Discussion

### 3.1. AHP Results

The different processes are shown in the following tables, where Table 5 presents the pair-wise assessment, Table 6 displays the normalization of these and Table 7 exhibits the weighted results of the AHP method, where specific heat capacity has a more significant importance in this application since this property absorbs heat and releases it.

Table 5. Comparison matrix of the criteria.

Criteria	Phase-Change Temp (°C)	Density (kg/m <sup>3</sup> )	Heat of Fusion (kJ/kg)	Specific Heat Capacity (kJ/kgK)	Thermal Conductivity (W/mK)	FOM1	FOM2
Phase-change Temp (°C)	1	3	3	0.33	0.33	0.33	0.33
Density (kg/m <sup>3</sup> )	0.33	1	0.2	0.20	0.33	0.33	0.33
Heat of fusion (kJ/kg)	0.33	5	1	0.33	0.33	1	1
Specific heat capacity (kJ/kgK)	3	5	3	1	3	3	3
Thermal conductivity (W/mK)	3	3	3	0	1	1	3
FOM1	3	3	1	0	1.00	1	1
FOM2	3	3	1	0	0.33	1	1
Summatory	13.67	23	12.20	2.87	6.33	7.67	9.67

Table 6. Normalized matrix of the criteria.

Phase-Change Temp (°C)	Density (kg/m <sup>3</sup> )	Heat of Fusion (kJ/kg)	Specific Heat Capacity (kJ/kgK)	Thermal Conductivity (W/mK)	FOM1	FOM2
0.0732	0.1304	0.2459	0.12	0.0526	0.04	0.03
0.0244	0.0435	0.0164	0.07	0.0526	0.04	0.03
0.0244	0.2174	0.0820	0.12	0.0526	0.13	0.10
0.2195	0.2174	0.2459	0.3488	0.4737	0.39	0.31
0.2195	0.1304	0.2459	0.12	0.1579	0.13	0.31
0.2195	0.1304	0.0820	0.1163	0.1579	0.13	0.10
0.2195	0.1304	0.0820	0.1163	0.0526	0.13	0.10

Table 7. Weighted criteria.

Criteria	Phase-Change Temp (°C)	Density (kg/m <sup>3</sup> )	Heat of Fusion (kJ/kg)	Specific Heat Capacity (kJ/kgK)	Thermal Conductivity (W/mK)	FOM1	FOM2
Compound	T1	T2	T3	T4	T5	T6	T7
Weight	0.099	0.041	0.104	0.315	0.187	0.134	0.119

Furthermore, the proof that the method was performed correctly is displayed in Table 8, in which the multiplication of the normalized matrix with the weighted matrix is calculated, allowing to subsequently calculate the consistency index (CI), the random index (RI) and consistency relationship (CR), displayed in Table 9. In this case, the consistency is less than 10%, proving that the weights were assessed correctly [34].

Table 8. Matrix multiplication.

	N × T	Priority/Weight
T1	0.785	7.89
T2	0.305	7.49
T3	0.761	7.33
T4	2.451	7.77
T5	1.516	8.10
T6	1.070	7.97
T7	0.945	7.93
Summatory		7.78

**Table 9.** Calculation of consistency.

Index	Value
CI	0.13
RI	1.32
CR	0.099

### 3.2. VIKOR Results

In previous research, the VIKOR method was found to be the best methodology for selection of materials in automotive applications, since this delivers a compromise set of solutions as the result [35]. In this sense, Table 10 shows the results of the calculations for the VIKOR method where the normalization takes place, taking in consideration the previous weights and the best and worst parameters.

**Table 10.** VIKOR calculations.

Compound	Phase-Change Temp (°C)	Density (kg/m <sup>3</sup> )	Heat of Fusion (kJ/kg)	Specific Heat Capacity (kJ/kgK)	Thermal Conductivity (W/mK)	FOM1	FOM2
M1	0.012	0.031	0.099	0.245	0	0.034	0.119
M2	0.025	0.032	0.101	0.199	0.022	0.042	0.081
M3	0.012	0.041	0.100	0.184	0.022	0.008	0.043
M4	0.037	0.016	0.070	0.245	0.148	0	0.020
M5	0.099	0.032	0.104	0.269	0.061	0.054	0.069
M6	0.050	0.011	0.074	0.245	0.144	0.044	0.051
M7	0.025	0.041	0.100	0	0.022	0.034	0.028
M8	0.037	0.011	0.074	0.199	0.144	0.044	0.040
M9	0.037	0.016	0.102	0.170	0.079	0.094	0.092
M10	0.037	0.014	0.092	0.245	0.144	0.074	0.035
M11	0	0.012	0.093	0.210	0.151	0.083	0.026
M12	0.037	0.012	0.095	0.047	0.151	0.086	0.000
M13	0	0.011	0.001	0.184	0.151	0.115	0.024
M14	0.012	0.011	0.000	0.194	0.151	0.117	0.025
M15	0.050	0	0.064	0.315	0.187	0.134	0.039

On the other hand, the ranking is displayed in Table 11, where savENRG PCM-HS22P stands as the best, being an organic PCM that is used in the storage of great energy and which has a low cost.

**Table 11.** VIKOR ranking.

Compound	Si	Ri	Qi	Ranking
M1	0.541	0.245	0.607	11
M2	0.502	0.199	0.463	6
M3	0.411	0.184	0.346	3
M4	0.537	0.245	0.603	10
M5	0.688	0.269	0.797	14
M6	0.619	0.245	0.679	12
M7	0.249	0.100	0	1
M8	0.548	0.199	0.506	8
M9	0.591	0.170	0.480	7
M10	0.642	0.245	0.701	13
M11	0.575	0.210	0.557	9
M12	0.428	0.151	0.285	2
M13	0.486	0.184	0.416	4
M14	0.510	0.194	0.460	5
M15	0.790	0.315	1.000	15

Furthermore, the verification of the method says that VIKOR performed well since  $Q_2 - Q_1 = 0.285$  is bigger than  $DQ = 0.17$ , showing an acceptable advantage. Furthermore, the results of  $S_i$  and  $R_i$  demonstrate that the best belongs to the winner M7, meaning that there is an acceptable stability, fulfilling the two conditions that conclude that the method has an acceptable compromised solution.

### 3.3. TOPSIS Results

The TOPSIS method, along with AHP, plays an important part to reduce a possible selection of a wrong PCM, which was also studied in the thermal management of electronics [36]. Moreover, the development of the normalized matrix, which takes the original criteria and divides them by the square root of the quadratic summation of all the materials, is shown in Table 12. In turn, the weighted matrix that multiplies the previous criteria by the AHP weight is displayed in Table 13, followed by the beneficial and non-beneficial solutions in Table 14. Lastly, the negative and positive ideal solutions with the closeness index for the ranking result is calculated in Table 15. In these results, again savENRG PCM-HS22P is the optimum material.

Table 12. TOPSIS normalized matrix.

Compound	Phase-Change Temp (°C)	Density (kg/m <sup>3</sup> )	Heat of Fusion (kJ/kg)	Specific Heat Capacity (kJ/kgK)	Thermal Conductivity (W/mK)	FOM1	FOM2
M1	0.275	0.335	0.214	0.231	0.440	0.312	0.401
M2	0.263	0.341	0.197	0.254	0.396	0.293	0.322
M3	0.275	0.406	0.208	0.261	0.396	0.368	0.244
M4	0.252	0.216	0.411	0.231	0.139	0.387	0.197
M5	0.195	0.340	0.180	0.220	0.316	0.267	0.298
M6	0.240	0.172	0.385	0.231	0.147	0.288	0.261
M7	0.263	0.406	0.208	0.353	0.396	0.312	0.213
M8	0.252	0.172	0.385	0.254	0.147	0.288	0.237
M9	0.252	0.212	0.191	0.268	0.279	0.177	0.346
M10	0.252	0.196	0.259	0.231	0.147	0.221	0.228
M11	0.286	0.181	0.254	0.249	0.132	0.200	0.207
M12	0.252	0.183	0.243	0.330	0.132	0.194	0.155
M13	0.286	0.175	0.169	0.261	0.132	0.129	0.204
M14	0.275	0.176	0.163	0.257	0.132	0.125	0.206
M15	0.240	0.089	0.221	0.197	0.059	0.086	0.236

Table 13. TOPSIS weighted matrix.

Compound	Phase-Change Temp (°C)	Density (kg/m <sup>3</sup> )	Heat of Fusion (kJ/kg)	Specific Heat Capacity (kJ/kgK)	Thermal Conductivity (W/mK)	FOM1	FOM2
M1	0.027	0.014	0.022	0.073	0.082	0.042	0.048
M2	0.026	0.014	0.020	0.080	0.074	0.039	0.038
M3	0.027	0.017	0.022	0.082	0.074	0.049	0.029
M4	0.025	0.009	0.043	0.073	0.026	0.052	0.023
M5	0.019	0.014	0.019	0.069	0.059	0.036	0.036
M6	0.024	0.007	0.040	0.073	0.027	0.039	0.031
M7	0.026	0.017	0.022	0.111	0.074	0.042	0.025
M8	0.025	0.007	0.040	0.080	0.027	0.039	0.028
M9	0.025	0.009	0.020	0.085	0.052	0.024	0.041
M10	0.025	0.008	0.027	0.073	0.027	0.030	0.027
M11	0.028	0.007	0.026	0.078	0.025	0.027	0.025
M12	0.025	0.007	0.025	0.104	0.025	0.026	0.018
M13	0.028	0.007	0.018	0.082	0.025	0.017	0.024
M14	0.027	0.007	0.017	0.081	0.025	0.017	0.025
M15	0.024	0.004	0.023	0.062	0.011	0.012	0.028

Table 14. Max and min TOPSIS criteria value.

Values +/-	Phase-Change Temp (°C)	Density (kg/m <sup>3</sup> )	Heat of Fusion (kJ/kg)	Specific Heat Capacity (kJ/kgK)	Thermal Conductivity (W/mK)	FOM1	FOM2
V+	0.028	0.004	0.043	0.111	0.082	0.052	0.018
V-	0.019	0.017	0.017	0.062	0.011	0.012	0.048

Table 15. TOPSIS Ranking.

Compound	Si+	Si-	Pi	Ranking
M1	0.054	0.079	0.593	4
M2	0.047	0.073	0.608	3
M3	0.040	0.079	0.663	2
M4	0.069	0.058	0.457	8
M5	0.060	0.056	0.482	5
M6	0.070	0.045	0.394	10
M7	0.029	0.089	0.755	1
M8	0.065	0.049	0.427	9
M9	0.059	0.050	0.458	7
M10	0.073	0.037	0.335	12
M11	0.073	0.039	0.345	11
M12	0.066	0.057	0.461	6
M13	0.078	0.037	0.322	13
M14	0.079	0.036	0.312	14
M15	0.098	0.025	0.201	15

### 3.4. COPRAS Method

The engineering fields have been benefiting from this method by enabling the decision maker to determine the overall efficiency of the different options [37]. In this way, the process of development is displayed in Table 16 with the normalized matrix that divides each position by the summation of all of them for every criterion. Table 17 presents the weighted matrix that is the result of the previous table by every weight of AHP, followed by Table 18 that shows the summation of the beneficial and non-beneficial weights. Lastly, the priority of positions with the level of performance and the COPRAS rank is presented in Table 19, where the results show that the material M7 savENRG PCM-HS22P again is established as the better material among the 15 candidates.

Table 16. COPRAS normalized table.

Compound	Phase-Change Temp (°C)	Density (kg/m <sup>3</sup> )	Heat of Fusion (kJ/kg)	Specific Heat Capacity (kJ/kgK)	Thermal Conductivity (W/mK)	FOM1	FOM2
M1	0.071	0.093	0.058	0.060	0.130	0.085	0.107
M2	0.068	0.095	0.053	0.066	0.117	0.080	0.086
M3	0.071	0.113	0.056	0.068	0.117	0.101	0.065
M4	0.065	0.060	0.111	0.060	0.041	0.106	0.052
M5	0.050	0.094	0.049	0.057	0.093	0.073	0.079
M6	0.062	0.048	0.104	0.060	0.043	0.079	0.069
M7	0.068	0.113	0.056	0.092	0.117	0.085	0.057
M8	0.065	0.048	0.104	0.066	0.043	0.079	0.063
M9	0.065	0.059	0.052	0.070	0.082	0.048	0.092
M10	0.065	0.055	0.070	0.060	0.043	0.061	0.061
M11	0.074	0.050	0.069	0.065	0.039	0.055	0.055
M12	0.065	0.051	0.066	0.086	0.039	0.053	0.041
M13	0.074	0.049	0.046	0.068	0.039	0.035	0.054
M14	0.071	0.049	0.044	0.067	0.039	0.034	0.055
M15	0.062	0.025	0.060	0.051	0.017	0.024	0.063

Table 17. COPRAS weighted matrix.

Compound	Phase-Change Temp (°C)	Density (kg/m <sup>3</sup> )	Heat of Fusion (kJ/kg)	Specific Heat Capacity (kJ/kgK)	Thermal Conductivity (W/mK)	FOM1	FOM2
M1	0.0071	0.0038	0.0060	0.0190	0.0243	0.0115	0.0127
M2	0.0068	0.0039	0.0055	0.0209	0.0219	0.0108	0.0102
M3	0.0071	0.0046	0.0059	0.0215	0.0219	0.0136	0.0078
M4	0.0065	0.0024	0.0116	0.0190	0.0077	0.0143	0.0062
M5	0.0050	0.0038	0.0051	0.0181	0.0174	0.0098	0.0095
M6	0.0062	0.0019	0.0108	0.0190	0.0081	0.0106	0.0083
M7	0.0068	0.0046	0.0059	0.0290	0.0219	0.0115	0.0068
M8	0.0065	0.0019	0.0108	0.0209	0.0081	0.0106	0.0075
M9	0.0065	0.0024	0.0054	0.0221	0.0154	0.0065	0.0110
M10	0.0065	0.0022	0.0073	0.0190	0.0081	0.0082	0.0072
M11	0.0074	0.0020	0.0072	0.0205	0.0073	0.0074	0.0066
M12	0.0065	0.0021	0.0068	0.0271	0.0073	0.0071	0.0049
M13	0.0074	0.0020	0.0048	0.0215	0.0073	0.0047	0.0065
M14	0.0071	0.0020	0.0046	0.0211	0.0073	0.0046	0.0065
M15	0.0062	0.0010	0.0062	0.0162	0.0032	0.0032	0.0075

Table 18. COPRAS solutions.

Compound	S <sup>+</sup> i	S <sup>-</sup> i
M1	0.068	0.017
M2	0.066	0.014
M3	0.070	0.012
M4	0.059	0.009
M5	0.055	0.013
M6	0.055	0.010
M7	0.075	0.011
M8	0.057	0.009
M9	0.056	0.013
M10	0.049	0.009
M11	0.050	0.009
M12	0.055	0.007
M13	0.046	0.008
M14	0.045	0.009
M15	0.035	0.009

Table 19. COPRAS ranking.

Compound	Qi	Ui	Rank
M1	0.074	88%	3
M2	0.074	87%	4
M3	0.079	93%	2
M4	0.071	85%	5
M5	0.064	75%	10
M6	0.065	77%	8
M7	0.085	100%	1
M8	0.068	81%	7
M9	0.064	76%	9
M10	0.060	72%	12
M11	0.062	74%	11
M12	0.070	83%	6
M13	0.058	69%	13
M14	0.057	68%	14
M15	0.048	56%	15

### 3.5. Spearman's Correlation Results

Table 20 shows the results of the Spearman's correlations where only the correlation COPRAS-TOPSIS has a very good relation; thus, the rest of them does not have a good relation although they indicate a positive correlation. However, it can be seen that the three methods show consistency in their results regarding the best material, as studied before [27].

**Table 20.** Spearman's correlation.

Correlation of 15 Materials Ranked			
	COPRAS	TOPSIS	VIKOR
COPRAS	-	0.914	0.439
TOPSIS	-	-	0.407

Moreover, even though the correlation shows that it is not perfect, it agrees with the fact that the material savENRG PCM-HS22P was chosen as the best, and since it is the one that will be simulated, Table 21 displays its properties.

**Table 21.** Selected material for simulation.

Compound	Phase-Change Temp (°C)	Density (kg/m <sup>3</sup> )	Heat of Fusion (kJ/kg)	Specific Heat Capacity (kJ/kgK)	Thermal Conductivity (W/mK)
savENRG PCM-HS22P	23	1540	185	3.05	0.54

Comparing the selection results with what Rastogi et al. had done, there is a difference where they prioritized the Figures of Merit since air conditioning systems require that the extraction of heat be primordial [25]. On the other hand, this application demands heat storage and release. Moreover, in the research of Socaciu et al., the best materials come from the same family as our best (SavEnrg PCM-Hs22P), also in thermal comfort applications in the automotive industry [38], corroborating that our selection is optimum.

### 3.6. Simulation Results

By reducing the difference in temperature between the internal air and body heat, the thermal comfort of the user can be controlled [39]. In this sense, the simulation with a raising temperature in the roof showed that without PCMs there is not much difference in the internal air, resulting in a high temperature in the cabin, as shown in Figure 2a. However, by using a 20 mm layer of the selected PCM, the temperature did not rise as much, and presented a decrease of near 9 °C, which is a congruent result compared with previous research that managed almost the same temperature degree with other PCMs [40–42]. This difference is showed in Figure 2b.

The discharging event, on the other hand, showed that while the temperature of the rooftop dropped to 12 °C, the internal air stood 4 °C warmer, meaning that the PCM maintain the internal comfort by releasing its stored energy into the cabin; this result is displayed in Figure 3.

Other researchers proved that the utilization of PCMs delayed the heat flux, making them more effective for isolation since the wall loses less energy, which helps to maintain a better temperature [9,43].

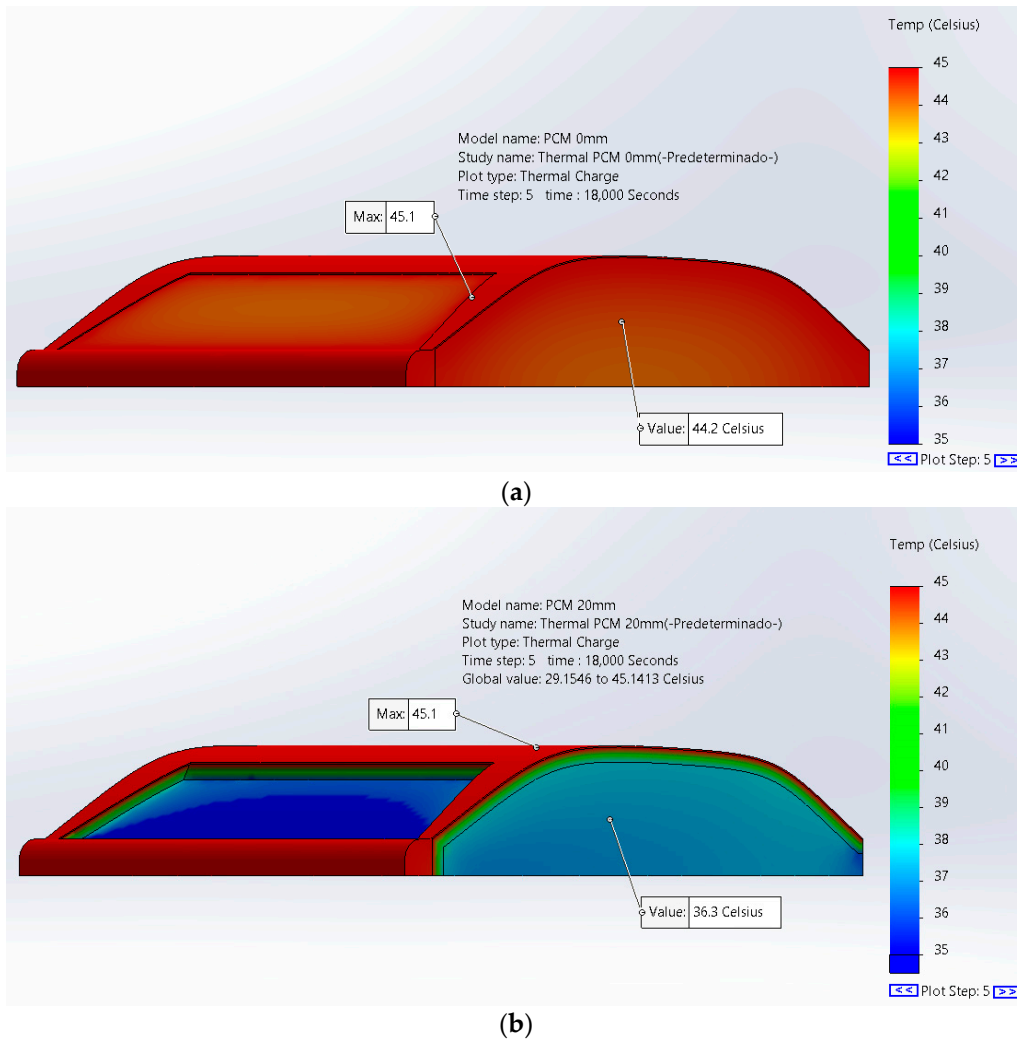


Figure 2. Charging the simulation comparison. (a) PCM 0 mm (b) PCM 20 mm.

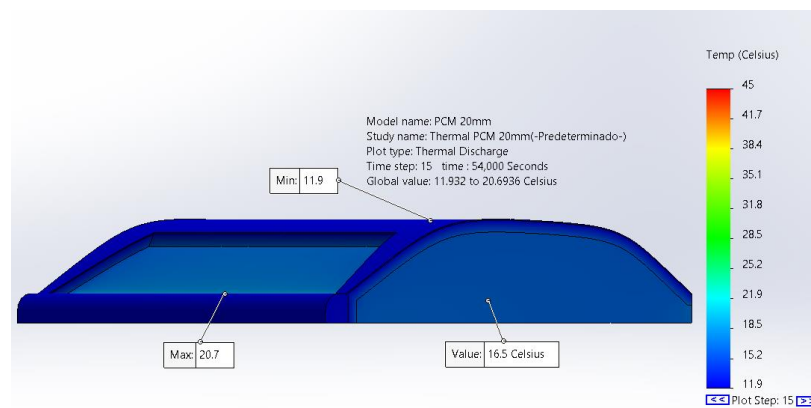


Figure 3. Discharge.

#### 4. Conclusions

Starting with a list of 15 PCMs, savENRG PCM-HS22P was selected as the best by the utilization of the AHP, VIKOR, COPRAS and TOPSIS multicriteria methods. Furthermore, a Spearman’s correlation showed that the methods are consistent, and the selection is optimum.

The simulation showed that the material savENRG PCM-HS22P improves the thermal comfort in the cabin by reducing the internal temperature of the air by 9 °C in the charging event, and in the discharging simulation it was also showed that the PCM allows to maintain a better temperature inside the cabin by making a differentiation of 4 °C warmer, both with a 20 mm layer of the selected PCM.

It is demonstrated that the use of a PCM layer of 20 mm can improve the thermal comfort in the vehicle, reducing the need to use the heater or the air conditioner.

**Author Contributions:** Conceptualization: J.M.-G. and J.F.N.; methodology: M.C., J.M.-G. and J.F.N.; software: M.C., J.M.-G. and J.F.N.; validation: M.C., J.M.-G., J.F.N., R.B.S. and E.R.; formal analysis: E.R., J.F.N. and J.M.-G.; investigation: E.R., J.F.N. and J.M.-G.; resources: E.R.; writing—original draft preparation: J.F.N.; writing—review and editing: E.R., R.B.S. and J.M.-G.; visualization: J.F.N.; supervision: J.M.-G.; project administration: J.M.-G.; funding acquisition: J.M.-G. All authors have read and agreed to the published version of the manuscript.

**Funding:** This research takes part of the project ‘Selection, characterization and simulation of phase change materials for thermal comfort, cooling and energy storage’. This project is part of the INEDITA call for R&D research projects in the field of energy and materials. This research is part of the project P121819, Parque de Energias Renovables, founded by Universidad Internacional SEK.

**Institutional Review Board Statement:** Not applicable.

**Informed Consent Statement:** Not applicable.

**Data Availability Statement:** The data reported in this research can be found at <https://drive.google.com/file/d/19rI2-2r6nYN0C3Ymjiegf55bdq4jrB8Z/view?usp=sharing> (accessed on 15 January 2021).

**Conflicts of Interest:** The authors declare that the research was conducted in the absence of any commercial or financial relationships that could be construed as a potential conflict of interest.

## References

1. Farrington, R.; Rugh, J. Impact of Vehicle Air-Conditioning on Fuel Economy, Tailpipe Emissions, and Electric Vehicle Range: Preprint. 2000. Available online: <https://www.osti.gov/biblio/764573> (accessed on 15 January 2021).
2. Antonijevic, D.; Heckt, R. Heat pump supplemental heating system for motor vehicles. *Proc. Inst. Mech. Eng. Part D J. Automob. Eng.* **2004**, *218*, 1111–1115. [[CrossRef](#)]
3. Kang, B.H.; Lee, H.J. A Review of Recent Research on Automotive HVAC Systems for EVs. *Int. J. Air-Cond. Refrig.* **2017**, *25*, 1730003. [[CrossRef](#)]
4. Simion, M.; Socaciu, L.; Unguresan, P. Factors which Influence the Thermal Comfort Inside of Vehicles. *Energy Procedia* **2016**, *85*, 472–480. [[CrossRef](#)]
5. Prajapati, D.G.; Kandasubramanian, B. Biodegradable Polymeric Solid Framework-Based Organic Phase-Change Materials for Thermal Energy Storage. *Ind. Eng. Chem. Res.* **2019**, *58*, 10652–10677. [[CrossRef](#)]
6. Jaguemont, J.; Omar, N.; Van den Bossche, P.; Mierlo, J. Phase-change materials (PCM) for automotive applications: A review. *Appl. Therm. Eng.* **2018**, *132*, 308–320. [[CrossRef](#)]
7. Nazir, H.; Batool, M.; Bolivar Osorio, F.J.; Isaza-Ruiz, M.; Xu, X.; Vignarooban, K.; Phelan, P.; Inamuddin; Kannan, A.M. Recent developments in phase change materials for energy storage applications: A review. *Int. J. Heat Mass Transf.* **2019**, *129*, 491–523. [[CrossRef](#)]
8. Kuznik, F.; Virgone, J. Experimental assessment of a phase change material for wall building use. *Appl. Energy* **2009**, *86*, 2038–2046. [[CrossRef](#)]
9. Liu, H.; Awbi, H.B. Performance of phase change material boards under natural convection. *Build. Environ.* **2009**, *44*, 1788–1793. [[CrossRef](#)]
10. Zhang, N.; Yuan, Y.; Cao, X.; Du, Y.; Zhang, Z.; Gui, Y. Latent Heat Thermal Energy Storage Systems with Solid–Liquid Phase Change Materials: A Review. *Adv. Eng. Mater.* **2018**, *20*, 1–30. [[CrossRef](#)]
11. Bakan, G.; Gerislioglu, B.; Dirisaglik, F.; Jurado, Z.; Sullivan, L.; Dana, A.; Lam, C.; Gokirmak, A.; Silva, H. Extracting the temperature distribution on a phase-change memory cell during crystallization. *J. Appl. Phys.* **2016**, *120*, 164504. [[CrossRef](#)]
12. Gerislioglu, B.; Bakan, G.; Ahuja, R.; Adam, J.; Mishra, Y.K.; Ahmadvand, A. The role of Ge<sub>2</sub>Sb<sub>2</sub>Te<sub>5</sub> in enhancing the performance of functional plasmonic devices. *Mater. Today Phys.* **2020**, *12*, 100178. [[CrossRef](#)]
13. Kuznik, F.; David, D.; Johannes, K.; Roux, J.J. A review on phase change materials integrated in building walls. *Renew. Sustain. Energy Rev.* **2011**, *15*, 379–391. [[CrossRef](#)]
14. Zhou, D.; Zhao, C.Y.; Tian, Y. Review on thermal energy storage with phase change materials (PCMs) in building applications. *Appl. Energy* **2012**, *92*, 593–605. [[CrossRef](#)]

15. Kim, K.; Choi, K.; Kim, Y.; Lee, K.; Lee, K. Feasibility study on a novel cooling technique using a phase change material in an automotive engine. *Energy* **2010**, *35*, 478–484. [CrossRef]
16. Yu, X.; Li, Z.; Lu, Y.; Huang, R.; Roskilly, A.P. Investigation of organic Rankine cycle integrated with double latent thermal energy storage for engine waste heat recovery. *Energy* **2019**, *170*, 1098–1112. [CrossRef]
17. Yang, K.; Zhu, N.; Chang, C.; Wang, D.; Yang, S.; Ma, S. A methodological concept for phase change material selection based on multi-criteria decision making (MCDM): A case study. *Energy* **2018**, *165*, 1085–1096. [CrossRef]
18. Amer, A.E.; Rahmani, K.; Lebedev, V.A. Using the Analytic Hierarchy Process (AHP) method for selection of phase change materials for solar energy storage applications. *J. Phys. Conf. Ser.* **2020**, *1614*, 12022. [CrossRef]
19. Mukhamet, T.; Kobeyev, S.; Nadeem, A.; Memon, S.A. Ranking PCMs for building façade applications using multi-criteria decision-making tools combined with energy simulations. *Energy* **2021**, *215*, 119102. [CrossRef]
20. Méndez, A.; Martínez-Gómez, J.; Rodríguez, F.; Nicolalde, J.F. Selección de un material de cambio de fase mediante el uso del método de selección multicriterio para su uso en un sistema de almacenamiento térmico automotriz. *RISTI Rev. Iber. Sist. Tecnol. Inf.* **2020**, 113–125. Available online: <https://www.proquest.com/openview/63deba1836c13b0f5ceb448dbcbfa2e3/1?pq-origsite=gscholar&cbl=1006393> (accessed on 15 January 2021).
21. Amoozad Mahdiraji, H.; Arzaghi, S.; Stauskis, G.; Zavadskas, E.K. A Hybrid Fuzzy BWM-COPRAS Method for Analyzing Key Factors of Sustainable Architecture. *Sustainability* **2018**, *10*, 1626. [CrossRef]
22. Shojaeefard, M.H.; Khalkhali, A.; Miandoabchi, E. Multi-criteria decision making approach for selecting the best friction distribution in superplastic forming of a vehicle component. *Proc. Inst. Mech. Eng. Part E J. Process Mech. Eng.* **2014**, *230*, 146–157. [CrossRef]
23. Singh, R.P.; Xu, H.; Kaushik, S.C.; Rakshit, D.; Romagnoli, A. Charging performance evaluation of finned conical thermal storage system encapsulated with nano-enhanced phase change material. *Appl. Therm. Eng.* **2019**, *151*, 176–190. [CrossRef]
24. Dhir, D.K. Thermo-mechanical performance of automotive disc brakes. *Mater. Today Proc.* **2018**, *5*, 1864–1871. [CrossRef]
25. Rastogi, M.; Chauhan, A.; Vaish, R.; Kishan, A. Selection and performance assessment of Phase Change Materials for heating, ventilation and air-conditioning applications. *Energy Convers. Manag.* **2015**, *89*, 260–269. [CrossRef]
26. Odu, G.O. Weighting methods for multi-criteria decision making technique. *J. Appl. Sci. Environ. Manag.* **2019**, *23*, 1449. [CrossRef]
27. Shekhovtsov, A.; Salabun, W. A comparative case study of the VIKOR and TOPSIS rankings similarity. *Procedia Comput. Sci.* **2020**, *176*, 3730–3740. [CrossRef]
28. Beltrán, R.D.; Martínez-Gómez, J. Analysis of phase change materials (PCM) for building wallboards based on the effect of environment. *J. Build. Eng.* **2019**, *24*, 100726. [CrossRef]
29. Mousavi-nasab, S.H.; Sotoudeh-anvai, A. A comprehensive MCDM-based approach using TOPSIS, COPRAS and DEA as an auxiliary tool for material selection problems. *Mater. Des.* **2017**, *121*, 237–253. [CrossRef]
30. Mousavi-Nasab, S.H.; Sotoudeh-Anvari, A. A new multi-criteria decision making approach for sustainable material selection problem: A critical study on rank reversal problem. *J. Clean. Prod.* **2018**, *182*, 466–484. [CrossRef]
31. Granta Design Limited. *CES-Edupack*; Granta Design Limited: Cambridge, UK, 2019.
32. Dadour, I.R.; Almanjahie, I.; Fowkes, N.D.; Keady, G.; Vijayan, K. Temperature variations in a parked vehicle. *Forensic Sci. Int.* **2011**, *207*, 205–211. [CrossRef]
33. Cengel, Y.; Boles, M.A. *Termodinámica*, 8th ed.; McGraw-Hill Interamericana: New York, NY, USA, 2015.
34. Nadeem, A.; Rakhman, K.; Hossain, M.A. Phase Change Materials Ranking by Using the Analytic Hierarchy Process. *Proc. Int. Struct. Eng. Constr.* **2020**, *7*, CPM-09-1–CPM-09-6. [CrossRef]
35. Jeya Girubha, R.; Vinodh, S. Application of fuzzy VIKOR and environmental impact analysis for material selection of an automotive component. *Mater. Des.* **2012**, *37*, 478–486. [CrossRef]
36. Kumar, A.; Kothari, R.; Sahu, S.K.; Kundalwal, S.I. Selection of phase-change material for thermal management of electronic devices using multi-attribute decision-making technique. *Int. J. Energy Res.* **2021**, *45*, 2023–2042. [CrossRef]
37. Chatterjee, P.; Athawale, V.M.; Chakraborty, S. Materials selection using complex proportional assessment and evaluation of mixed data methods. *Mater. Des.* **2011**, *32*, 851–860. [CrossRef]
38. Socaci, L.; Giurgiu, O.; Banyai, D.; Simion, M. PCM selection using AHP method to maintain thermal comfort of the vehicle occupants. *Energy Procedia* **2016**, *85*, 489–497. [CrossRef]
39. Holmer, I.; Nilsson, H.; Bohm, M.; Noren, O. Thermal Aspects of Vehicle Comfort. *Appl. Hum. Sci.* **1995**, *14*, 159–165. [CrossRef]
40. Purusothaman, M.; Saichand, K.; Sam Cornilius, C.; Siva, R. Experimental Investigation of Thermal Performance in a Vehicle Cabin Test Setup with Pcm in the Roof. In *IOP Conference Series: Materials Science and Engineering*; IOP Publishing: Bristol, UK, 2017. [CrossRef]
41. Saleel, C.A.; Mujeebu, M.A.; Algarni, S. Coconut oil as phase change material to maintain thermal comfort in passenger vehicles. *J. Therm. Anal. Calorim.* **2019**, *136*, 629–636. [CrossRef]
42. Oró, E.; de Jong, E.; Cabeza, L.F. Experimental analysis of a car incorporating phase change material. *J. Energy Storage* **2016**, *7*, 131–135. [CrossRef]
43. Arıcı, M.; Bilgin, F.; Nižetić, S.; Karabay, H. PCM integrated to external building walls: An optimization study on maximum activation of latent heat. *Appl. Therm. Eng.* **2020**, *165*, 114560. [CrossRef]